Biochemical and Biophysical Research Communications 440 (2013) 235–240

Contents lists available at ScienceDirect

Biochemical and Biophysical Research Communications

journal homepage: www.elsevier.com/locate/ybbrc

The effect of the adaptor protein Isd11 on the quaternary structure of the eukaryotic cysteine desulphurase Nfs1

Kerem Teralı [a,1], Rebecca L. Beavil [b], Richard W. Pickersgill [a,*], Mark van der Giezen [c,*]

[a] School of Biological and Chemical Sciences, Queen Mary University of London, Mile End Road, London E1 4NS, UK
[b] Randall Division of Cell and Molecular Biophysics, King's College London, New Hunt's House, Guy's Campus, London SE1 1UL, UK
[c] Biocatalysis Centre, Biosciences, College of Life & Environmental Sciences, University of Exeter, Stocker Road, Exeter EX4 4QD, UK

ARTICLE INFO

Article history:
Received 3 September 2013
Available online 14 September 2013

Keywords:
Iron–sulphur (Fe–S) cluster assembly
Mitochondria
Saccharomyces cerevisiae
Nfs1
Isd11

ABSTRACT

Small inorganic assemblies of alternating ferrous/ferric iron and sulphide ions, so-called iron–sulphur (Fe–S) clusters, are possibly nature's most ancient prosthetic groups. One of the early actors in Fe–S cluster biosynthesis is a protein complex composed of a cysteine desulphurase, Nfs1, and its functional binding partner, Isd11. Although the essential function of Nfs1·Isd11 in the liberation of elemental sulphur from free cysteine is well established, little is known about its structure. Here, we provide evidence that shows Isd11 has a profound effect on the oligomeric state of Nfs1.

1. Introduction

Iron–sulphur (Fe–S) clusters, which are composed of iron and inorganic sulphide, are likely to be the earliest cofactors available for enzyme catalysis, holding a mirror to naturally occurring oxidation and reduction reactions in the context of prebiotic chemistry [1]. Protein-bound Fe–S clusters are found in virtually all biological systems where they participate in a number of processes including electron transfer, biosynthesis, central metabolism, regulation of gene expression, RNA modification, and DNA repair and replication [2–4]. Fe–S clusters can be synthesised *in vitro*, starting with an iron source (Fe^{2+}) and elemental sulphur (S^0) [5]. The low solubility of Fe^{3+} ion and high toxicity of free Fe^{2+} and S^{2-} ions within the cell, however, have caused organisms to develop elaborate mechanisms that promote: (i) the donation of iron and sulphur in a non-toxic form; (ii) the *de novo* assembly of a transient Fe–S cluster on a molecular scaffold; and (iii) the delivery of the pre-assembled cluster from the scaffold to a recipient apoprotein.

In the eukaryotic system, functioning of the proteinaceous iron–sulphur cluster (ISC) assembly machinery, which is conserved throughout eukaryotes, is central to the biosynthesis of Fe–S clusters. Components of the eukaryotic ISC assembly machinery are derived from their prokaryotic counterparts and originally arrived with the endosymbiont that gave rise to the mitochondrion [6]. The ISC assembly machinery still primarily, or exclusively, localises to mitochondria. An early crucial reaction in mitochondrial Fe–S cluster assembly involves sulphur abstraction from free cysteine, with subsequent transfer to the Isu1 scaffold protein. This reaction is catalysed by a protein complex comprising Nfs1 and Isd11. Nfs1 is a pyridoxal-5′-phosphate (PLP)-dependent cysteine desulphurase belonging to the class V aminotransferase family of proteins (Pfam entry PF00266). The corresponding open reading frame (YCL017c) was first discovered when the entire DNA sequence of *Saccharomyces cerevisiae* chromosome III was determined [7]. The gene product was named Nfs1 for bearing a certain degree of sequence similarity to NifS of nitrogen-fixing bacteria. Only sometime after the identification of a NifS-like protein in a eukaryote, Dean and co-workers reported that NifS from the nitrogen-fixing bacterium *Azotobacter vinelandii* existed as a PLP-containing homodimer and catalysed the conversion of L-cysteine into L-alanine, sequestering the released sulphur atom in the form of a protein-bound persulphide intermediate on a conserved cysteinyl residue [8,9]. The same catalytic mechanism for L-cysteine desulphuration was subsequently described for IscS, another NifS-like protein, from *Escherichia coli* [10]. NifS from the hypertermophilic bacterium *Thermotaga maritima* was the first NifS-like protein of which the crystal structure was reported to a resolution of 2.0 Å [11]. *T. maritima* NifS (PDB entry 1ECX) is a dimer of two identical subunits, each of which is divided into a small and a large domain. The active site lies close to the surface near the dimer interface and harbours the PLP cofactor covalently attached through a Schiff-base linkage to a conserved lysinyl residue (Lys203), forming an internal aldimine. The catalytic cysteinyl residue (Cys324) resides in the middle of a 12-residue-long highly flexible loop. Stacking

* Corresponding authors.
E-mail addresses: r.w.pickersgill@qmul.ac.uk (R.W. Pickersgill), m.vandergiezen@exeter.ac.uk (M. van der Giezen).
[1] Current address: Turkish Cypriot DNA Laboratory, Dr. Burhan Nalbantoğlu State Hospital, Nicosia 99010, Cyprus.

0006-291X/$ - see front matter © 2013 Elsevier Inc. All rights reserved.
http://dx.doi.org/10.1016/j.bbrc.2013.09.039

on top of PLP is a conserved histidinyl residue (His99) which is proposed to serve as an acid/base catalyst during the reaction. The crystal structure of *T. maritima* NifS was followed by the crystal structure of IscS from *E. coli* to a resolution of 2.1 Å [12].

Until recently, Nfs1 was thought to catalyse sulphur delivery to the Isu1 scaffold protein by itself. This, however, was disproved by two independent groups of workers who reported that *S. cerevisiae* Nfs1 required binding of a small (11 kDa) protein called Isd11 to fulfil its regular function [13,14]. Isd11 is assigned to the LYR family (Pfam entry PF05347), which is named for the presence of a conserved leucine–tyrosine–arginine tripeptide motif near the N-terminus of its protein members. The corresponding open reading frame (YER048w-a) resides on yeast chromosome V [15]. Comparative analysis of sequenced genomes revealed that Isd11 was exclusive to eukaryotes including mitosomal and hydrogenosomal lineages. The absence of Isd11 in currently available prokaryotic genomes directly implies that Isd11 is a eukaryotic supplement to the bacterium-derived ISC assembly apparatus [16].

In addition to their central mission in Fe–S cluster formation, both Nfs1 and Isd11 appear to be responsible for the regulation of iron metabolism. Yeast cells depleted of Nfs1 [17] or Isd11 [13] showed an increase in mitochondrial iron content, as compared with the wild-type cells. Mitochondrial iron overload is a characteristic of a group of human diseases, which are associated with deficient Fe–S cluster assembly proteins (e.g., frataxin-deficient Friedreich's ataxia). It is widely known that the essential nature of iron as an outstanding biological catalyst may also result in the generation of highly toxic hydroxyl radicals via the Fenton reaction, reflecting the double-edged role of this metal in the cell. This makes Nfs1 and Isd11 potential candidates for disease pathology.

Native Nfs1·Isd11 from yeast is estimated to be about 180–200 kDa in size [13], with no clue as to its subunit stoichiometry. Moreover, in the context of Fe–S cluster assembly, the exact molecular and structural function of Isd11 as a binding partner of Nfs1 remains elusive. To address these issues, we produced soluble yeast Nfs1 in isolation as well as in complex with yeast Isd11 in *E. coli*. Both Nfs1 and the Nfs1·Isd11 complex bind L-cysteine, indicating that the recombinantly produced proteins correspond to their *in vivo* counterparts. Our results show that Nfs1 adopts a higher oligomeric state in the Isd11-bound form compared to that in the free form.

2. Materials and methods

2.1. Production and purification of Nfs1 and the Nfs1·Isd11 complex

S. cerevisiae Nfs1 and Isd11 were produced in *E. coli* RosettaBlue(DE3)pLysS cells and the Nfs1·Isd11 complex was produced in *E. coli* RosettaBlue(DE3) cells. The individual genes were cloned into pET-14b (Novagen) and the two genes together into pCDFDuet-1 (Novagen). The constructs were designed to introduce hexahistidine tags at the N-terminal end of the resulting proteins and to exclude the predicted mitochondrial targeting sequences (residues 1–34 of Nfs1 and residues 1–10 of Isd11) from the resulting proteins [18]. The nucleotide sequences of the final constructs were confirmed by sequencing. Purification of Nfs1 and of the Nfs1·Isd11 complex was by immobilised metal affinity chromatography, followed by size exclusion chromatography [19].

2.2. Homology modelling of Nfs1

Model building was achieved using the semi-automated MODELLER 9v7 program (http://www.salilab.org/modeller/), which employed the satisfaction-of-spatial-restraints method. The quality of the model was checked and confirmed by superimposing the model structure on the template structure using PyMOL (http://www.pymol.org) and manually inspecting the active site.

2.3. Quantitative amino acid analysis of the Nfs1·Isd11 complex

A sample of Nfs1·Isd11 in 4 mM HEPES, 40 mM NaCl, 0.2 mM DTT, 0.2 mM EDTA, and 1% (v/v) glycerol, pH 7.0 was sent to the Protein and Nucleic Acid Chemistry Facility at the University of Cambridge for quantitative amino acid analysis.

2.4. Analytical ultracentrifugation of the Nfs1·Isd11 complex

The sedimentation equilibrium experiment was set up with three different concentrations (A_{280} = 0.8, A_{280} = 0.6 and A_{280} = 0.4) of the freshly purified Nfs1·Isd11 protein complex. Each sample was loaded in a separate analytical cell of an Optima XL-A analytical ultracentrifuge (Beckman Coulter) and run at three different rotor speeds (7000 rpm, 8500 rpm and 10,000 rpm) at 4 °C, producing a total of nine data sets. Analytical ultracentrifugation parameters (ρ, $\bar{v}_{Nfs1}$ and $\bar{v}_{Isd11}$) were computed using the SEDNTERP program (http://www.rasmb.bbri.org/software/). Computed molecular mass of each subunit was entered manually. Data were fitted using the SigmaPlot software (Systat). Residuals were calculated by subtracting the best fit of the model from the experimental data. A random distribution of the residuals around zero was noted as a function of the radius.

2.5. Spectroscopic measurements

UV–visible absorbance and fluorescence emission spectra were recorded at 25 °C on, respectively, a U-3010 absorbance spectrophotometer and an F-2500 fluorescence spectrophotometer (both Hitachi) using 3.65 mg ml^{-1} protein in 20 mM HEPES, 200 mM NaCl, 1 mM DTT, 1 mM EDTA, 5% (v/v) glycerol, pH 7.0. Far-UV CD spectra were recorded at 25 °C on a Chirascan spectropolarimeter (Applied Photophysics) using 0.12 mg ml^{-1} protein in 2.5 mM HEPES, 25 mM NaCl, pH 7.0. Spectral deconvolution was performed using the dedicated K2D3 web server (http://www.ogic.ca/projects/k2d3/).

2.6. Substrate-binding assay

The activities of purified Nfs1 and Nfs1·Isd11 were assayed *in vitro* by adding free L-cysteine at a final concentration of 10 mM (incubation allowed at 4 °C) and monitoring the reaction by UV–visible absorbance spectrophotometry. Cysteine desulphurase activity was measured in terms of the decrease in A_{420} as a function of time.

3. Results and discussion

3.1. Recombinantly produced Isd11 accumulates as inclusion bodies and does not readily refold

When produced in *E. coli*, yeast Isd11 exhibited an absolute tendency to form inclusion bodies (data not shown). Isd11 could be solubilised using chaotropic agents, but on their removal the protein was again insoluble.

3.2. Recombinantly produced Nfs1 is a PLP-binding homodimer

Overnight incubation of the IPTG-induced *E. coli* cells harbouring the pET-based construct resulted in high levels of soluble Nfs1 (Supplemental Fig. 1A). The recombinant protein was bright yellow and the presence of protein-bound PLP was confirmed by

UV–visible absorbance spectrophotometry in which a typical absorption band centred at 420 nm appeared (Supplemental Fig. 1B). Size-exclusion chromatography suggested that recombinant Nfs1 had an apparent molecular mass of approximately 100 kDa, which corresponds to the size of the homodimer. This finding is consistent with the previous studies on the characterisation of the oligomeric state of cysteine desulphurases [8,10–12,20].

Homology modelling provided detailed insight into the integrity of the active site of yeast Nfs1. Among all available molecular structures representing NifS-like proteins, *E. coli* IscS (PDB entry 1P3 W) was identified as the best structural template for modelling the eukaryotic enzyme. The proposed homodimeric Nfs1 model has a very similar fold to that of IscS, with both α-helical and β-stranded secondary structures conserved (Fig. 1A). The PLP cofactor is anchored in the active site of Nfs1 via formation of an internal aldimine Schiff base with Lys299 as well as a number of hydrogen bonds (Fig. 1B). Asp239 and Gln242 help stabilising the position of the pyridine ring of PLP, while Thr135, Ser262 and His264 help stabilising the position of its phosphate group in the active site. The catalytic cysteinyl residue, Cys328, of *E. coli* IscS is located in the middle of a 10-residue-long flexible loop (GSA**C**TSASLE) which is directed away from the active site [12]. This residue corresponds to Cys421 in yeast Nfs1 and is proposed to act as a nucleophile to attack the sulphydryl group of the PLP-bound l-cysteine substrate, forming a protein-bound cysteinyl persulphide intermediate. As the flexible loop harbouring Cys328 is missing from the crystal structure of IscS, no attempt was made to model the position of the catalytic cysteinyl residue, though it is clearly within reach of the active centre.

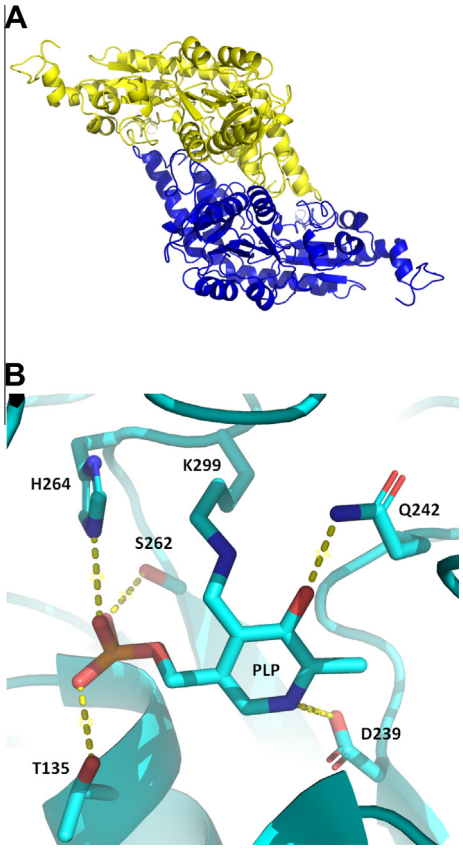

Fig. 1. Homology modelling of Nfs1. (A) Ribbon structure of Nfs1, seen looking down the two-fold axis. A greater portion of the polypeptide backbone adopts an α-helical conformation. The two monomers are shown in yellow and blue. This image was rendered using PyMOL (http://www.pymol.org). (B) Cartoon representation of the active site of yeast Nfs1, with PLP and the PLP-binding residues shown in stick representation. The PLP cofactor makes a covalent link to Lys299. Polar interactions, stabilising the position of PLP in the active site, are indicated by yellow dashed lines. This image was rendered using PyMOL (http://www.pymol.org). (For interpretation of the references to colour in this figure legend, the reader is referred to the web version of this article.)

3.3. Nfs1 and the Nfs1·Isd11 complex are active toward L-cysteine

The activities of recombinantly produced Nfs1 and Nfs1·Isd11 were assayed by incubating each protein with a high molar excess of free L-cysteine and following the displacement reaction between L-cysteine and PLP by UV–visible absorbance spectrophotometry. Because the substrate was used in high molar excess, the system displayed absorption bands corresponding to all long-living species (Fig. 2). Ideally, DTT in the system reacts with the enzyme-bound persulphide, regenerating the active-site cysteinyl residue and liberating sulphur in the S^{2-} redox state [21]. Upon addition of L-cysteine, the intensity of the absorption band at 420 nm, which is assigned to the protonated internal aldimine, decreases with a concomitant increase of absorbance at 330 nm or 336 nm, the former for Nfs1 and the latter for Nfs1·Isd11. The newly formed absorbing species corresponds to the crucial L-cysteine –PLP ketimine adduct, on which the reactive cysteine thiolate performs a nucleophilic attack to cleave the C–S bond and form the enzyme-bound cysteinyl persulphide intermediate (Cys–S–SH) and an enamine derivative of L-alanine [22]. The change in absorbance at 420 nm (or 330/336 nm) is considerable for the first 5-min interval, but then in subsequent 5-min intervals the activity reduces. Clearly, the internal aldimine is not being regenerated, or else the peak at 420 nm would persist. Therefore, it is likely that only a single turnover is being monitored during the course of the experiment. It may be that the high concentration of the substrate added (10 mM) competes with the catalytic cysteinyl residue, leading to a trapped substrate–PLP ketimine adduct. Alternatively, the substrate could form a disulphide linkage with the cysteinyl residue on the flexible loop of Nfs1, preventing it from accepting the sulphur cargo, again trapping the ketimine. In either case, it is clear that the enzyme-bound PLP is reacting with free L-cysteine and forming the ketimine, revealing that the active centre of the recombinant enzyme is correctly formed. The UV–visible absorbance spectrophotometric data show that the Nfs1·Isd11 complex follows the same reaction scheme as Nfs1 and its bacterial homologues. Interestingly, Nfs1, when incubated for several hours with L-cysteine, precipitated out of solution, as judged visually (data not shown). Nfs1·Isd11, however, showed no signs of precipitation after the same time.

3.4. There is a rearrangement of Nfs1 in the Nfs1·Isd11 complex compared to Nfs1 alone

To characterise the secondary structure of the recombinantly produced proteins, the far-UV CD spectroscopic signal of Nfs1 alone and in complex with Isd11 were measured. The CD data were normalised by calculating the mean residue ellipticity, $[\theta]_{mrw}$, allowing spectra in the far-UV region to be directly compared for Nfs1 and the Nfs1·Isd11 complex (mean residue weight considered to be 115 Da). The far-UV CD spectrum of Nfs1, with two strong negative troughs at 208 nm and 222 nm, represents a typical circular dichroic pattern for a compact globular protein having extensive α-helical content (Fig. 3A). The K2D3 algorithm estimates that 56% of the amino acid residues adopt an α-helical conformation and that 13% of the amino acid residues adopt a β-stranded conformation [23]. This prediction is in agreement with the previous reports on the X-ray crystallographic studies of the prokaryotic NifS-like proteins [11,12]. Calculated fractions of α-helix and β-strand contents of Nfs1·Isd11 from the given spectrum are, respectively, 20% and 28%. Although secondary-structure prediction tools point to the predominantly α-helical nature of Isd11

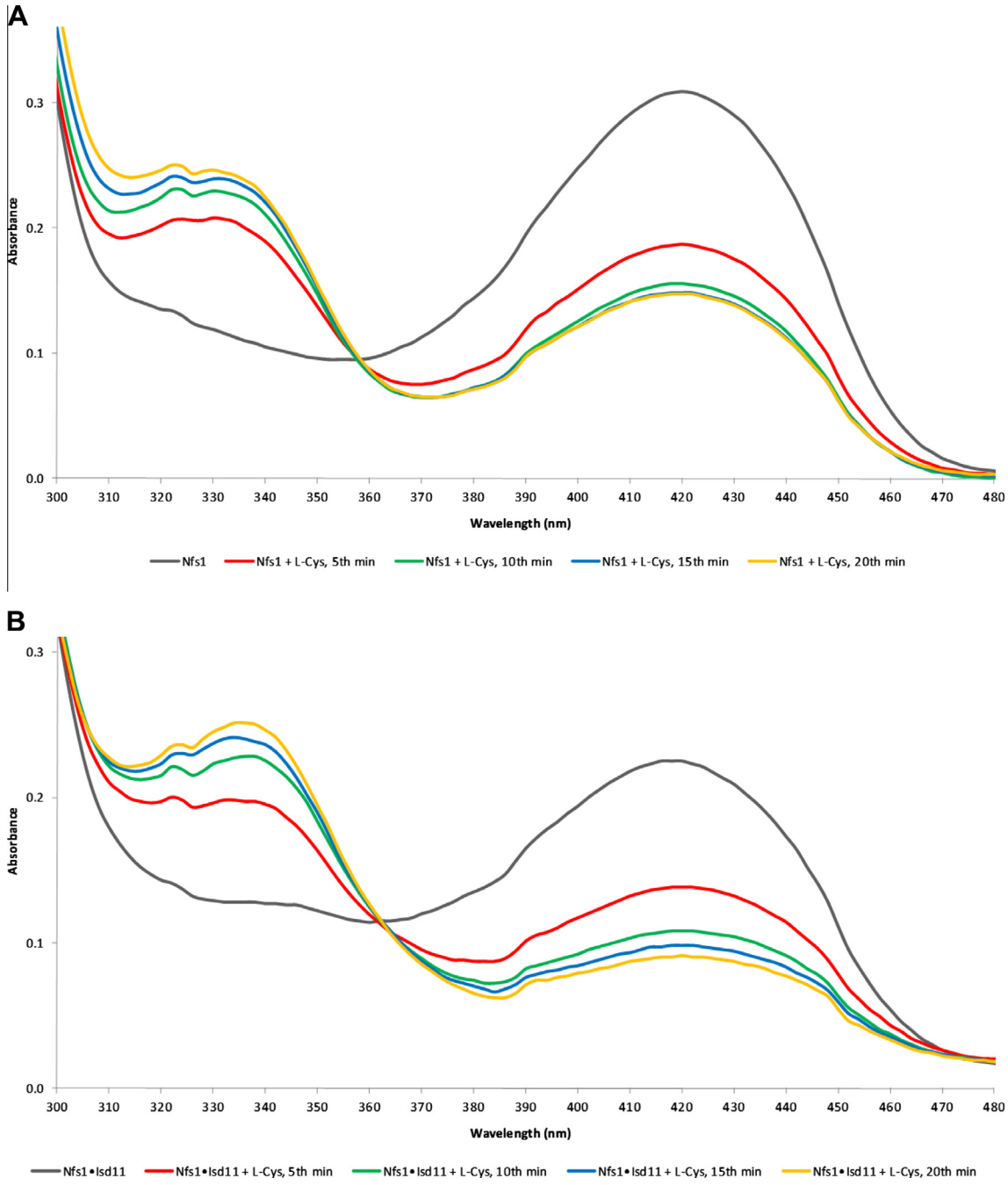

Fig. 2. Both Nfs1 and Nfs1·Isd11 are able to bind L-cysteine in a PLP-dependent manner. (A) Time-dependent spectral analysis of L-cysteine binding to Nfs1. Addition of free cysteine leads to a loss of absorption at 420 nm. Simultaneously, a second reaction intermediate absorbing at 330 nm is populated. (B) Time-dependent spectral analysis of L-cysteine binding to Nfs1·Isd11. Addition of free cysteine results in a decrease of absorption at 420 nm and a concomitant increase of absorption at 336 nm.

[16], far-UV CD spectroscopy indicates a decrease in the helical content and an increase in the strand content of Nfs1 in complex with Isd11. While the possibility exists that Isd11 may adopt a β-stranded conformation, its contribution to the signal must be small compared with that of Nfs1, which is roughly five times the size of Isd11. This phenomenon can be explained by the fact that complex formation sometimes results in a marked change in the spectroscopic signal even when the estimated contents of secondary structural elements remain essentially same [24]. Therefore, changes in the far-UV CD spectrum of the Nfs1·Isd11 protein complex are likely to reflect alterations in the orientation of helices with respect to each other rather than the actual helical content. These CD changes suggest a substantial rearrangement of the Nfs1 subunits in the Isd11-bound form compared to that in the free form.

We also measured the emission spectra of Nfs1 both in isolation and in complex with Isd11 to obtain further evidence for the structural effect of Isd11 on Nfs1. The intrinsic fluorescence measurements presented in this study exploit the fact that yeast Isd11 contains no tryptophanyl residues, while yeast Nfs1 contains three tryptophanyl residues. Upon Isd11 binding, the emission maximum for Nfs1 shifts from 348 nm to 343 nm, indicating that one or more tryptophanyl residues become less exposed to the aqueous buffer (Fig. 3B). With Isd11 bound, intrinsic tryptophan fluorescence also quenches by 21%, which is possibly due to the varying interaction of the tryptophanyl residues with peptide

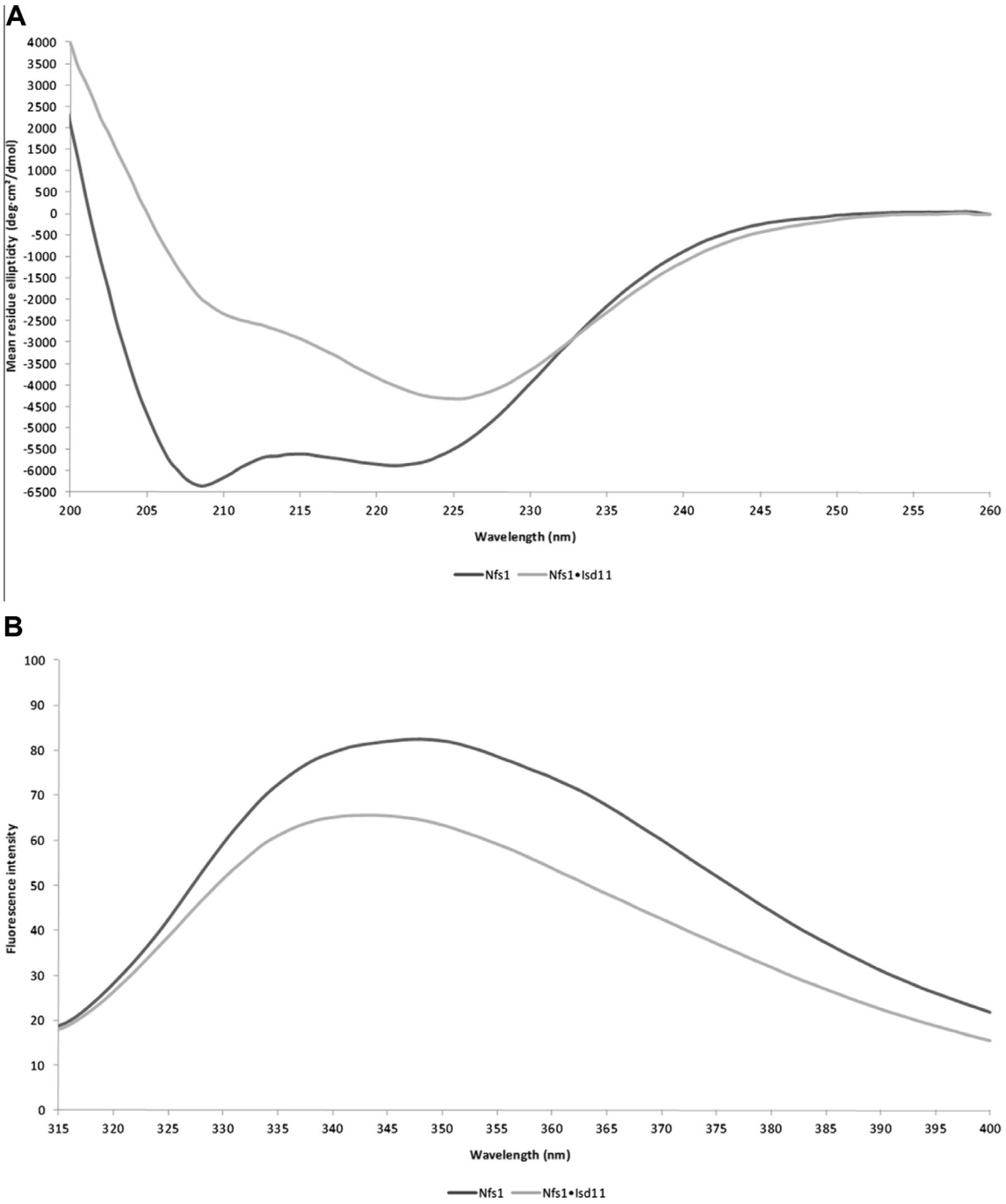

Fig. 3. Isd11 induces a substantial change in Nfs1 upon binding. (A) Comparison of the far-UV CD spectra of Nfs1 and Nfs1·Isd11. Binding of Isd11 leads to a considerable loss of the CD signal at 208 nm, with a moderate loss at 222 nm. (B) Comparison of the emission spectra of Nfs1 and the Nfs1·Isd11 complex. Upon complex formation, the intensity of Nfs1 fluorescence quenches, and the emission band shifts to a lower wavelength.

bonds and a number of amino acid side chains in the new macromolecular architecture. These findings suggest that the buried tryptophanyl residue is normally situated in the Nfs1–Isd11 binding site and/or the binding of Isd11 promotes a rearrangement of the Nfs1 subunits such that the tryptophanyl residue becomes more buried.

3.5. The Nfs1·Isd11 complex is a trimer of Nfs1–Isd11 heterodimers

Coexpression of *nfs1* and *isd11* in the same *E. coli* cell allowed the generation of a high-molecular-mass soluble protein complex containing Nfs1 and Isd11 in stoichiometric amounts (Supplemental Fig. 2). Quantitative amino acid analysis of the whole complex was used to determine the relative ratio of the constituent subunits. From comparison of the average variance contributions of reliable amino acid residues for each of the three possible repeating units ($Nfs1_2$–Isd11, Nfs1–Isd11 or Nfs1–$Isd11_2$), Nfs1 is most likely to interact with Isd11 in a molar ratio of 1:1 (Supplemental Table 1). Sedimentation-equilibrium analytical ultracentrifugation was used to characterise the quaternary structure of the Nfs1·Isd11 protein complex. A total of nine data sets were fitted to a range of mathematical models where the accuracy of each fit was judged by the residuals and statistics. The best fit was obtained for a non-interacting two-species model as described previously [25]. The corresponding residuals were randomly distributed around zero, supporting the proposed model. The results

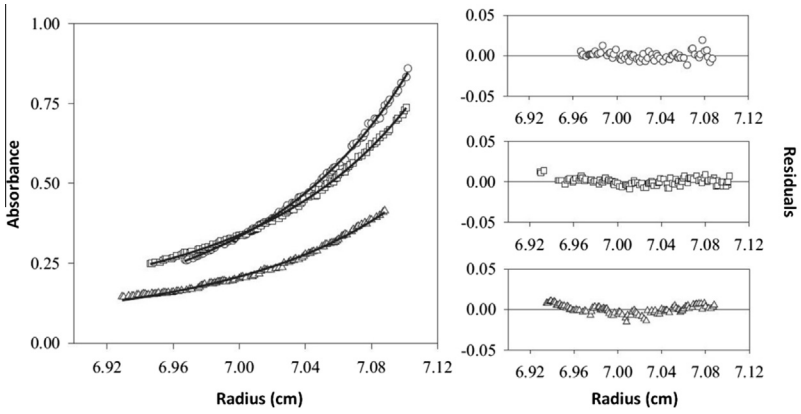

Fig. 4. Biophysical characterisation of yeast Nfs1·Isd11. Sedimentation equilibrium profile at 280 nm, and the corresponding residuals, for the Nfs1·Isd11 complex run at 8500 rpm. The experimental data are best described by a model comprising $(Nfs1–Isd11)_3$ and a smaller non-interacting component. Loading concentrations are shown in different symbols, as: A_{280} of 0.8 is indicated by circles; A_{280} of 0.6 is indicated by squares; A_{280} of 0.4 is indicated by triangles.

from analytical ultracentrifugation suggest that the sample was a mixture of mostly the $(Nfs1–Isd11)_3$ heterohexamer with residual non-interacting material of fixed molecular mass (approximately one-third the size of the $(Nfs1–Isd11)_3$ heterohexamer), which could be a degradation product (Fig. 4). The existence of the $(Nfs1–Isd11)_3$ heterohexamer was confirmed by size exclusion chromatography, which indicated that the recombinant complex had an apparent molecular mass of approximately 190 kDa. Three Isd11 molecules therefore bring three Nfs1 subunits together, most plausibly in a trimer of Nfs1–Isd11 heterodimers. The whole process could be mediated by allosteric binding behaviour and protein–protein interactions, as in the case of formation of the heterohexameric Tim9·Tim10 complex of the mitochondrial inter-membrane space [26]. The Isd11-binding-induced Nfs1 oligomerisation phenomenon is in agreement with the CD spectroscopic changes, which suggest a substantial change in the architecture of the Nfs1·Isd11 complex compared to Nfs1 alone. This may represent a remarkable control of the activity of Nfs1 as compared to bacterial cysteine desulphurases.

Acknowledgments

K.T. is grateful for a 3 year full-time Queen Mary University of London PhD Studentship. M.v.d.G. is grateful for support from the University of Exeter and Queen Mary University of London. R.W.P. acknowledges support from HEFCE and Queen Mary University of London.

Appendix A. Supplementary data

Supplementary data associated with this article can be found, in the online version, at http://dx.doi.org/10.1016/j.bbrc.2013.09.039.

References

[1] D.C. Rees, J.B. Howard, The interface between the biological and inorganic worlds: iron–sulfur metalloclusters, Science 300 (2003) 929–931.
[2] R. Lill, R. Dutkiewicz, H.P. Elsässer, A. Hausmann, D.J.A. Netz, A.J. Pierik, O. Stehling, E. Urzica, U. Mühlenhoff, Mechanisms of iron–sulfur protein maturation in mitochondria, cytosol and nucleus of eukaryotes, Biochim. Biophys. Acta 1763 (2006) 652–667.
[3] R. Lill, U. Mühlenhoff, Maturation of iron–sulfur proteins in eukaryotes: mechanisms, connected processes, and diseases, Annu. Rev. Biochem. 77 (2008) 669–700.
[4] A. Sheftel, O. Stehling, R. Lill, Iron–sulfur proteins in health and disease, Trends Endocrinol. Metab. 21 (2010) 302–314.
[5] H. Beinert, R.H. Holm, E. Münck, Iron–sulfur clusters: nature's modular, multipurpose structures, Science 277 (1997) 653–659.
[6] R. Lill, U. Mühlenhoff, Iron–sulfur-protein biogenesis in eukaryotes, Trends Biochem. Sci. 30 (2005) 133–141.
[7] S.G. Oliver, Q.J. van der Aart, M.L. Agostoni-Carbone, M. Aigle, L. Alberghina, D. Alexandraki, G. Antoine, R. Anwar, J.P. Ballesta, P. Benit, et al., The complete DNA sequence of yeast chromosome III, Nature 357 (1992) 38–46.
[8] L. Zheng, R.H. White, V.L. Cash, R.F. Jack, D.R. Dean, Cysteine desulfurase activity indicates a role for NIFS in metallocluster biosynthesis, Proc. Natl. Acad. Sci. USA 90 (1993) 2754–2758.
[9] L. Zheng, R.H. White, V.L. Cash, D.R. Dean, Mechanism for the desulfurization of L-cysteine catalyzed by the nifS gene product, Biochemistry 33 (1994) 4714–4720.
[10] D.H. Flint, *Escherichia coli* contains a protein that is homologous in function and N-terminal sequence to the protein encoded by the nifS gene of *Azotobacter vinelandii* and that can participate in the synthesis of the Fe–S cluster of dihydroxy-acid dehydratase, J. Biol. Chem. 271 (1996) 16068–16074.
[11] J.T. Kaiser, T. Clausen, G.P. Bourenkow, H.D. Bartunik, S. Steinbacher, R. Huber, Crystal structure of a NifS-like protein from *Thermotoga maritima*: implications for iron sulphur cluster assembly, J. Mol. Biol. 297 (2000) 451–464.
[12] J.R. Cupp-Vickery, H. Urbina, L.E. Vickery, Crystal structure of IscS, a cysteine desulfurase from *Escherichia coli*, J. Mol. Biol. 330 (2003) 1049–1059.
[13] A.C. Adam, C. Bornhövd, H. Prokisch, W. Neupert, K. Hell, The Nfs1 interacting protein Isd11 has an essential role in Fe/S cluster biogenesis in mitochondria, EMBO J. 25 (2006) 174–183.
[14] N. Wiedemann, E. Urzica, B. Guiard, H. Muller, C. Lohaus, H.E. Meyer, M.T. Ryan, C. Meisinger, U. Muhlenhoff, R. Lill, N. Pfanner, Essential role of Isd11 in mitochondrial iron–sulfur cluster synthesis on Isu scaffold proteins, EMBO J. 25 (2006) 184–195.
[15] F.S. Dietrich, J. Mulligan, K. Hennessy, M.A. Yelton, E. Allen, R. Araujo, E. Aviles, A. Berno, T. Brennan, J. Carpenter, et al., The nucleotide sequence of *Saccharomyces cerevisiae* chromosome V, Nature 387 (1997) 78–81.
[16] T.A. Richards, M. van der Giezen, Evolution of the Isd11/IscS complex reveals a single α-proteobacterial endosymbiosis for all eukaryotes, Mol. Biol. Evol. 23 (2006) 1341–1344.
[17] J. Li, M. Kogan, S.A.B. Knight, D. Pain, A. Dancis, Yeast mitochondrial protein, Nfs1p, coordinately regulates iron–sulfur cluster proteins, cellular iron uptake, and iron distribution, J. Biol. Chem. 274 (1999) 33025–33034.
[18] M.G. Claros, P. Vincens, Computational method to predict mitochondrially imported proteins and their targeting sequences, Eur. J. Biochem. 241 (1996) 779–786.
[19] K. Terali, Characterisation of the yeast Nfs1/Isd11 cysteine desulphurase complex. Ph.D. Thesis [online], Queen Mary, University of London, UK, (2010) <http://qmro.qmul.ac.uk/jspui/handle/123456789/572>.
[20] U. Mühlenhoff, J. Balk, N. Richhardt, J.T. Kaiser, K. Sipos, G. Kispal, R. Lill, Functional characterization of the eukaryotic cysteine desulfurase Nfs1p from *Saccharomyces cerevisiae*, J. Biol. Chem. 279 (2004) 36906–36915.
[21] M. Fontecave, S. Ollagnier-de-Choudens, Iron–sulfur cluster biosynthesis in bacteria: mechanisms of cluster assembly and transfer, Arch. Biochem. Biophys. 474 (2008) 226–237.
[22] E. Behshad, J.M. Bollinger Jr., Kinetic analysis of cysteine desulfurase CD0387 from *Synechocystis* sp. PCC 6803: formation of the persulfide intermediate, Biochemistry 48 (2009) 12014–12023.
[23] C. Louis-Jeune, M.A. Andrade-Navarro, C. Perez-Iratxeta, Prediction of protein secondary structure from circular dichroism using theoretically derived spectra, Proteins 80 (2012) 374–381.
[24] S.M. Kelly, N.C. Price, Circular dichroism to study protein interactions, Curr. Protoc. Protein Sci. (2006) Chapter 20, Unit 20 10.
[25] J. Shi, R. Ghirlando, R.L. Beavil, A.J. Beavil, M.B. Keown, R.J. Young, R.J. Owens, B.J. Sutton, H.J. Gould, Interaction of the low-affinity receptor CD23/FcεRII lectin domain with the Fcε3–4 fragment of human immunoglobulin E, Biochemistry 36 (1997) 2112–2122.
[26] E. Ivanova, H. Lu, Allosteric and electrostatic protein–protein interactions regulate the assembly of the heterohexameric Tim9–Tim10 complex, J. Mol. Biol. 379 (2008) 609–616.